

## Article

# Silicon Oxide Etching Process of $\text{NF}_3$ and $\text{F}_3\text{NO}$ Plasmas with a Residual Gas Analyzer

Woo-Jae Kim <sup>1</sup>, In-Young Bang <sup>1</sup>, Ji-Hwan Kim <sup>1</sup>, Yeon-Soo Park <sup>1</sup>, Hee-Tae Kwon <sup>1</sup>, Gi-Won Shin <sup>1</sup>, Min-Ho Kang <sup>2</sup>, Youngjun Cho <sup>3</sup>, Byung-Hyang Kwon <sup>3</sup>, Jung-Hun Kwak <sup>3</sup> and Gi-Chung Kwon <sup>1,\*</sup>

<sup>1</sup> Department of Electrical and Biological Physics, Kwangwoon University, 20 Kwangwoon-ro, Nowon-gu, Seoul 01897, Korea; dnwo424@naver.com (W.-J.K.); bebe403@naver.com (I.-Y.B.); oneaeo@daum.net (J.-H.K.); small2008@naver.com (Y.-S.P.); HeeTae\_Kwon@outlook.com (H.-T.K.); swat2100@naver.com (G.-W.S.)

<sup>2</sup> Department of Nano-Process, National Nanofab Center (NNFC), 291 Daehak-ro, Yuseong-gu, Daejeon 34141, Korea; kmh@nnfc.re.kr

<sup>3</sup> SK Materials Co., Ltd., 110-5, Myeonghaksandan-ro, Yeondong-myeon, Sejong 30068, Korea; choyongjun@sk.com (Y.C.); qudgid@sk.com (B.-H.K.); jhkwak@sk.com (J.-H.K.)

\* Correspondence: gckwon@kw.ac.kr

**Abstract:** The use of  $\text{NF}_3$  is significantly increasing every year. However,  $\text{NF}_3$  is a greenhouse gas with a very high global warming potential. Therefore, the development of a material to replace  $\text{NF}_3$  is required.  $\text{F}_3\text{NO}$  is considered a potential replacement to  $\text{NF}_3$ . In this study, the characteristics and cleaning performance of the  $\text{F}_3\text{NO}$  plasma to replace the greenhouse gas  $\text{NF}_3$  were examined. Etching of  $\text{SiO}_2$  thin films was performed, the DC offset of the plasma of both gases (i.e.,  $\text{NF}_3$  and  $\text{F}_3\text{NO}$ ) was analyzed, and a residual gas analysis was performed. Based on the analysis results, the characteristics of the  $\text{F}_3\text{NO}$  plasma were studied, and the  $\text{SiO}_2$  etch rates of the  $\text{NF}_3$  and  $\text{F}_3\text{NO}$  plasmas were compared. The results show that the etch rates of the two gases have a difference of 95% on average, and therefore, the cleaning performance of the  $\text{F}_3\text{NO}$  plasma was demonstrated, and the potential benefit of replacing  $\text{NF}_3$  with  $\text{F}_3\text{NO}$  was confirmed.

**Keywords:** nitrogen oxide trifluoride; nitrogen fluoride oxide; reactive ion etch; silicon oxide etch



**Citation:** Kim, W.-J.; Bang, I.-Y.; Kim, J.-H.; Park, Y.-S.; Kwon, H.-T.; Shin, G.-W.; Kang, M.-H.; Cho, Y.; Kwon, B.-H.; Kwak, J.-H.; et al. Silicon Oxide Etching Process of  $\text{NF}_3$  and  $\text{F}_3\text{NO}$  Plasmas with a Residual Gas Analyzer. *Materials* **2021**, *14*, 3026. <https://doi.org/10.3390/ma14113026>

Academic Editor: Alenka Vesel

Received: 8 April 2021

Accepted: 30 May 2021

Published: 2 June 2021

**Publisher's Note:** MDPI stays neutral with regard to jurisdictional claims in published maps and institutional affiliations.



**Copyright:** © 2021 by the authors. Licensee MDPI, Basel, Switzerland. This article is an open access article distributed under the terms and conditions of the Creative Commons Attribution (CC BY) license (<https://creativecommons.org/licenses/by/4.0/>).

## 1. Introduction

Since the 1980s, the use of  $\text{NF}_3$  plasmas in semiconductor, display, and solar cell processing applications has been investigated [1].  $\text{NF}_3$  plasma is used to etch various thin films under reactive ion etching (RIE) conditions [2,3] or to clean a plasma-enhanced chemical vapor deposition (PECVD) chamber [4,5]. Cleaning the PECVD chamber is performed by supplying ions and radicals for cleaning through a remote plasma source (RPS) [6] or by directly supplying ions and radicals through an in situ plasma discharge [7]. In addition,  $\text{NF}_3$  is attracting attention as a new etching technology, such as cryogenic electron beam induced etching (EBIE) [8,9] and highly selective etching [10].  $\text{NF}_3$  has a high etch rate, etching efficiency, and a relatively high chemical stability [2,11]. Accordingly, the use of  $\text{NF}_3$  is significantly increasing every year. However,  $\text{NF}_3$  is a greenhouse gas with a very high global warming potential of 16,100 and a lifespan of 500 years [12]. The contribution of  $\text{NF}_3$  to the radiative forcing in the Earth's atmosphere is very small, ~0.01%, in 2011, but the use of  $\text{NF}_3$  is increasing every day; therefore, this number continues to increase [13]. The share of  $\text{NF}_3$  in fluorinated gases increased from 13–28% in 2005 to 17–36% in 2010, and  $\text{NF}_3$  is currently the most widely used and released fluorinated gas [1,14]. Thus, it was included in the second commitment period of the Kyoto Protocol as the seventh greenhouse gas whose emissions are to be regulated [15].

Studies have been conducted to replace  $\text{NF}_3$  [16,17]. Among them,  $\text{F}_3\text{NO}$  was considered a candidate gas to replace  $\text{NF}_3$  [18]. Similar to  $\text{NF}_3$ ,  $\text{F}_3\text{NO}$  does not contain perfluorocarbons. In addition, because its molecule has an N=O bond, its atmospheric life

is relatively short, and thus, its contribution to global warming is expected to be less than that of  $\text{NF}_3$ . The etch rate of  $\text{F}_3\text{NO}$  is almost the same as that of  $\text{NF}_3$ . However, further studies on  $\text{F}_3\text{NO}$  have not been conducted, and information on the mechanism occurring in the  $\text{F}_3\text{NO}$  plasma during the cleaning process is insufficient. Therefore, research on the  $\text{F}_3\text{NO}$  plasma to replace  $\text{NF}_3$  is urgently needed.

The present study focused on evaluating and analyzing the properties of  $\text{F}_3\text{NO}$  plasma. Accordingly, the cleaning abilities of  $\text{NF}_3$  and  $\text{F}_3\text{NO}$  were compared, and the characteristics of the  $\text{F}_3\text{NO}$  plasma were analyzed. The cleaning ability of the  $\text{F}_3\text{NO}$  plasma was evaluated by etching a  $\text{SiO}_2$  film previously deposited on a Si wafer sample. Although the etching time of the small sample and the cleaning time of the PECVD chamber may not coincide, it was considered suitable for the evaluation of the cleaning ability of the gas. To analyze the etch mechanism, the etching plasma was diagnosed using a residual gas analyzer (RGA) and a high-voltage probe. The reactions in the  $\text{F}_3\text{NO}$  plasma were predicted by comparing the types and intensity of ions generated in the  $\text{NF}_3$  and  $\text{F}_3\text{NO}$  plasmas. In addition, the etch rates of the  $\text{SiO}_2$  thin film using the  $\text{NF}_3$  and  $\text{F}_3\text{NO}$  plasmas were compared to confirm whether the  $\text{F}_3\text{NO}$  plasma can replace  $\text{NF}_3$ .

## 2. Materials and Methods

The plasma etching equipment used in this study is shown in Figure 1. We manufactured the RIE equipment with a direct capacitively coupled plasma chamber to measure the plasma etching characteristics. The detailed geometry of the device has been shown in a previous study [19]. A coolant path was formed in the electrode, which was designed to maintain a constant temperature ( $15\text{ }^\circ\text{C}$ ) during the process.

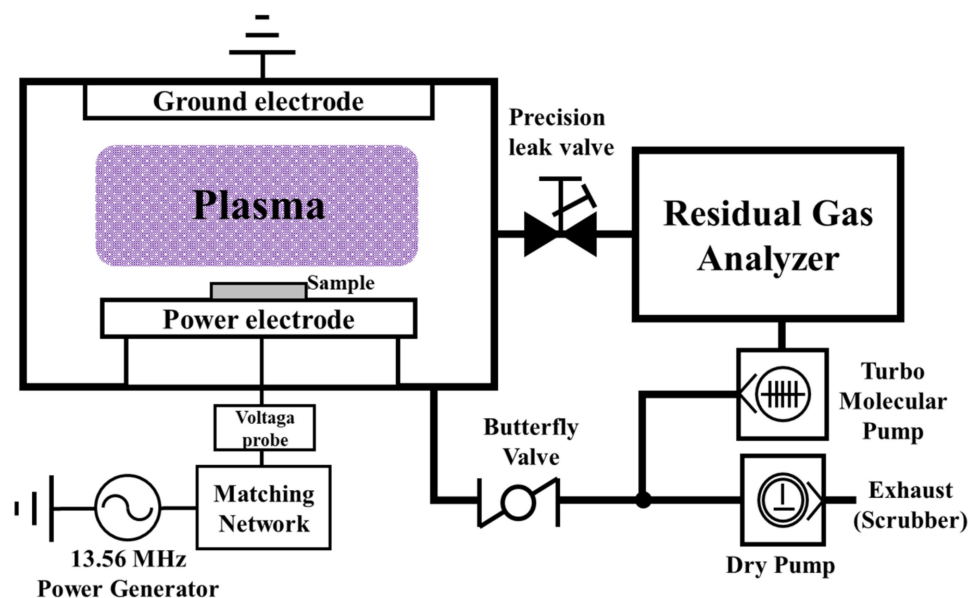


Figure 1. Plasma etching equipment setup.

The sample used for etching was a  $\text{SiO}_2$  thin film deposited on a Si wafer. The size of the sample was  $30\text{ mm} \times 30\text{ mm}$ , and the thickness of the thin film was  $2\text{ }\mu\text{m}$ .  $\text{NF}_3$  and  $\text{F}_3\text{NO}$  were used as process gases for etching. The  $\text{F}_3\text{NO}$  used in the experiments was manufactured and supplied by SK Materials (Sejong, Korea) and the National NanoFab Center (Daejeon, Korea). The purity of the provided  $\text{F}_3\text{NO}$  gas was 99.995%. The injected process gas was controlled using mass flow controllers. The process flow rate was fixed at 120 sccm. After the injection of the process gas, the process pressure was adjusted using a butterfly valve. The working pressure range was 130–270 mTorr. This working pressure range was set to confirm the possibility of cleaning in situ with a small amount of gas in the chamber while reducing the amount of cleaning gas without any additional high

flow MFC configuration. After reaching the process pressure, the discharge power was applied through the RF power generator. The RF input power range was 240–400 W, and the process time was fixed at 3 min.

Mass spectrometry measurements were performed using an RGA (RGA 300, SRS, Sunnyvale, CA, USA). As shown in Figure 1, the RGA is equipped with a differential pump system. The pressure of the differential pump system was fixed at 0.8 mTorr regardless of the process pressure. At this time, the ionization energy of the RGA was fixed at 70 eV. The DC self-bias (DC offset) was measured using a high-voltage probe to determine the characteristics of the  $\text{NF}_3$  and  $\text{F}_3\text{NO}$  plasmas. The etching rate of the thin film was evaluated after etching by measuring its thickness using the spectroscopic reflectometry method via the S-TRC series (Wonwoo Systems Co., Ltd., Seoul, Korea) [20].

### 3. Results and Discussion

To compare the characteristics of the  $\text{NF}_3$  and  $\text{F}_3\text{NO}$  plasmas and to understand the characteristics of the latter, a DC offset measurement during the RIE plasma discharge was performed (Figure 2). The  $\text{F}_3\text{NO}$  plasma showed a similar DC offset value very close to that of the  $\text{NF}_3$  plasma.

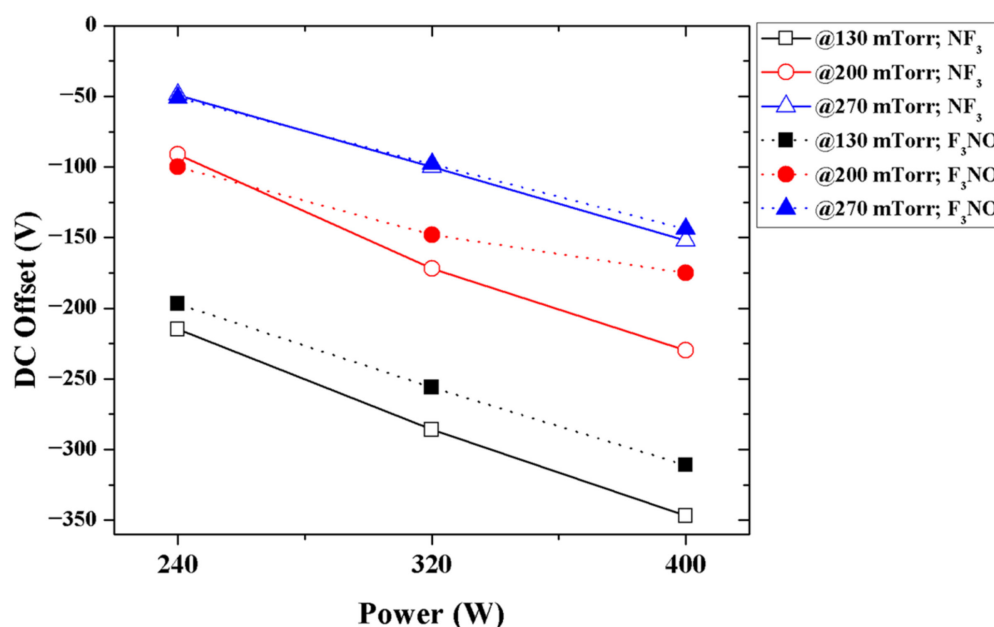


Figure 2. DC offset of the RF electrode during plasma discharge at a total flow rate of 120 sccm.

The  $\text{NF}_3$  plasma has a very high electronegativity [21,22]. Therefore, when compared with fluorocarbon plasmas, the  $\text{NF}_3$  plasma shows a relatively low DC offset value. Plasma with a high electronegativity tends to be unstable and easily collapses. In this case, the  $\text{NF}_3$  plasma is discharged only in a part of the chamber, and the plasma collapses in other parts; therefore, these parts may not be exposed to the plasma. Alternatively, a constant discharge may not occur but may flicker and cause discharge.

The comparison results of the DC offset of the  $\text{NF}_3$  and  $\text{F}_3\text{NO}$  plasmas show that the electronegativity of the  $\text{F}_3\text{NO}$  plasma can also be quite considerable. In the case of the  $\text{NF}_3$  plasma, an inert gas (e.g., He, Ar) was diluted and discharged to increase the stability and uniformity of the plasma and enhance etch rates [23–26]. Inert gases rarely participate in chemical reactions in the plasma but can have a great influence on the discharge process. The DC offset result indicates that the characteristics of the  $\text{F}_3\text{NO}$  plasma can also be comparable to those of the  $\text{NF}_3$  plasma. Thus, in future studies, dilution with an inert gas, such as Ar, is recommended.

Figure 3 shows the current of  $\text{F}^+$  ions and etch products ( $\text{SiF}$ ,  $\text{SiF}_2$ , and  $\text{SiF}_3$ ) generated from the  $\text{NF}_3$  and  $\text{F}_3\text{NO}$  plasmas when etching  $\text{SiO}_2$  thin films. As the pressure and power

increased, the intensity of the peak of F ions and the etch product also increased. At this time, when the pressure or discharge power was low, more F ions were generated in the  $F_3NO$  plasma than in the  $NF_3$  plasma. In addition, the lower the discharge power, the higher the generation of etch products in  $F_3NO$  than in  $NF_3$ . These findings confirmed that the etching of  $F_3NO$  occurs more actively at low power and pressure. In addition, as the power increases, the intensity of F ions in  $NF_3$  rapidly increases, whereas in the  $F_3NO$  plasma, the F ions gradually increase even if the discharge power of F increases. As will be shown further, this trend is similar for other ions as well. Consequently, the plasma density of  $F_3NO$  reacts more slowly to the change of the discharge power compared to  $NF_3$ .

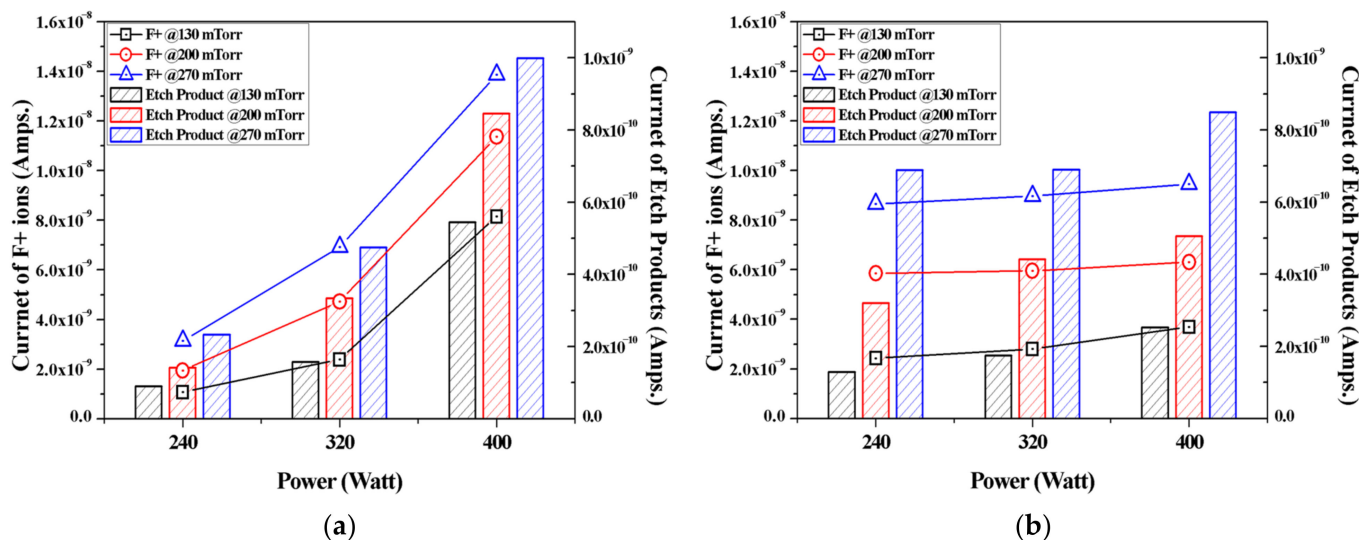


**Figure 3.** (a) Intensity of F+ ions and the sum of the etch product ions (SiF+, SiF<sub>2</sub>+, and SiF<sub>3</sub>+) during  $NF_3$  plasma silicon oxide etching as functions of the input power for various working pressures; (b) Intensity of F+ ions and the sum of the etch product ions (SiF+, SiF<sub>2</sub>+, and SiF<sub>3</sub>+) during  $F_3NO$  plasma silicon oxide etching as functions of the input power for various working pressures.

Among the ions generated in the  $NF_3$  and  $F_3NO$  plasmas during the silicon oxide thin film etching, O and O<sub>2</sub> were more common in the  $F_3NO$  plasma under all conditions (Figure 4). Compared with the  $F_3NO$  plasma, O and O<sub>2</sub> ions hardly occurred in the  $NF_3$  plasma. In the case of the  $F_3NO$  plasma, O and O<sub>2</sub> ions were simultaneously generated by O contained in  $F_3NO$  and O<sub>2</sub> gas already present in the chamber, whereas the  $NF_3$  plasma generated O and O<sub>2</sub> ions only from O<sub>2</sub> gas existing in the base. Therefore, when the pressure increased, the intensity of O and O<sub>2</sub> ions generated in the  $NF_3$  plasma was almost unchanged, whereas in the  $F_3NO$  plasma, when the pressure increased, O and O<sub>2</sub> ions appeared to rapidly increase compared to the  $NF_3$  plasma.

Figure 5 shows the peak intensities of the major ions generated in the  $NF_3$  and  $F_3NO$  plasmas during the etching of a silicon oxide thin film. N, N<sub>2</sub>, and F<sub>2</sub> ions occurred more in  $F_3NO$  at low discharging powers and more in  $NF_3$  at higher discharging powers. Conversely, NF<sub>2</sub> ions occurred more in the  $NF_3$  plasma under all conditions.

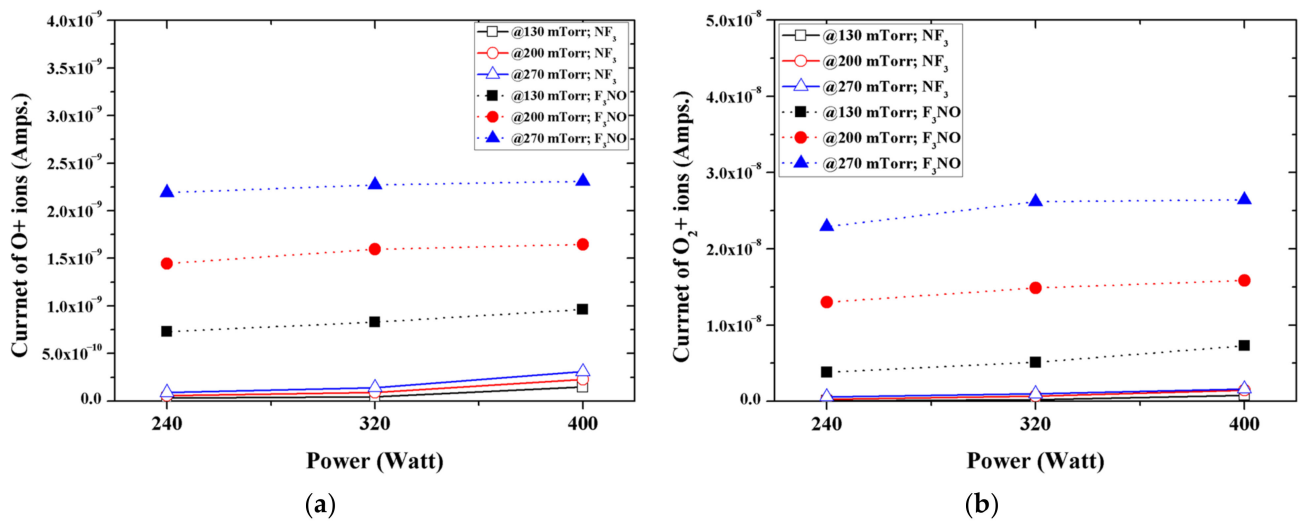


Figure 4. Intensity of: (a) O<sup>+</sup> ions; (b) O<sub>2</sub><sup>+</sup> during plasma silicon oxide etching as functions of input power for various working pressures.

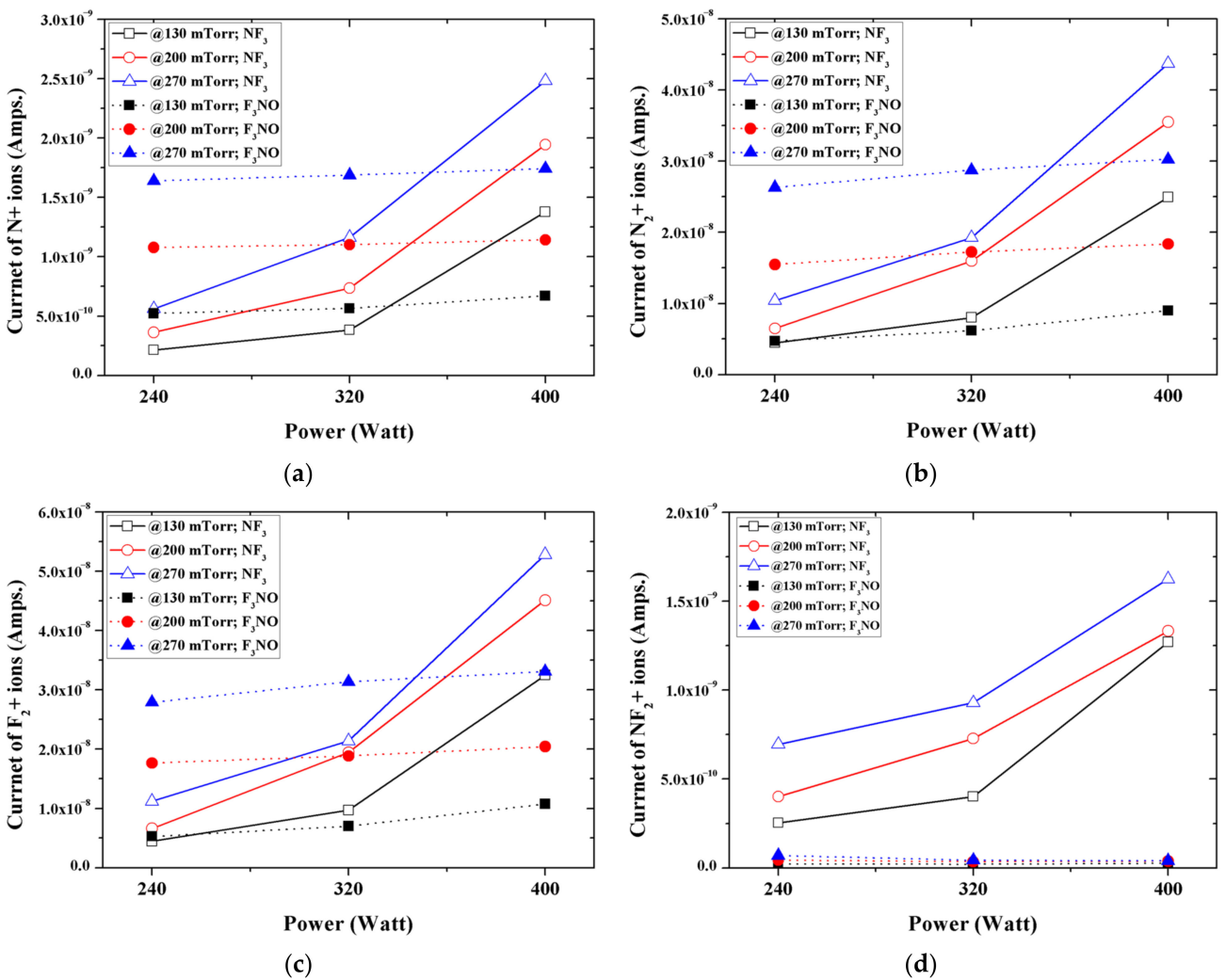
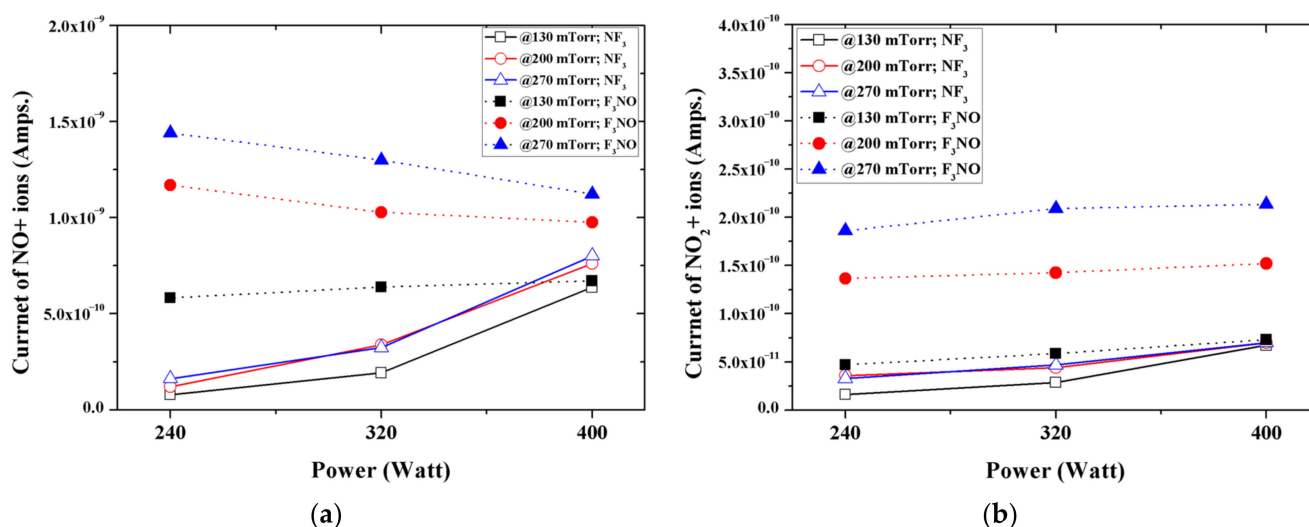


Figure 5. Intensity of: (a) N<sup>+</sup> ions; (b) N<sub>2</sub><sup>+</sup> ions; (c) F<sub>2</sub><sup>+</sup> ions; (d) NF<sub>2</sub><sup>+</sup> ions during plasma silicon oxide etching as functions of the input power for various working pressures.



Figure 6 shows the intensity of NO and NO<sub>2</sub> ions generated in the NF<sub>3</sub> and F<sub>3</sub>NO plasmas during the etching of silicon oxide thin films. When the discharge power was low, the NO ions generated in the F<sub>3</sub>NO plasma were more than those of the NF<sub>3</sub> plasma (numerical value). However, as the discharge power increased, the number of NO ions in the F<sub>3</sub>NO plasma gradually decreased, whereas those in the NF<sub>3</sub> plasma rapidly increased and became almost the same as the peak intensity of NO ions generated in the F<sub>3</sub>NO plasma. Conversely, many more NO<sub>2</sub> ions occurred in the F<sub>3</sub>NO plasma under all conditions.

In the NF<sub>3</sub> and F<sub>3</sub>NO plasmas, NO was produced through the following reaction :  $N_2 (A^3\Sigma_u^+)$  O  $\rightarrow$  NO + N. (1)



**Figure 6.** Intensity: of (a) NO<sup>+</sup> ions; (b) NO<sub>2</sub><sup>+</sup> ions during plasma silicon oxide etching as functions of the input power for various working pressures.

Metastable N<sub>2</sub> is produced mostly by collisions with a high-energy electron, making the mechanism more significant in an electronegative gas discharge, such as NF<sub>3</sub> and F<sub>3</sub>NO. At a higher discharge power, higher energy electrons are supplied, thus increasing the density of NO ions [27]:

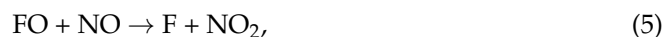


A reaction involving atomic nitrogen that resulted in a different density of NO ions in the F<sub>3</sub>NO plasma and the NF<sub>3</sub> plasma was more important in an oxygen-rich plasma [28,29]. As shown in Figure 4a, because F<sub>3</sub>NO is an oxygen-rich plasma, reaction (2) became significant, and a large amount of NO ions were produced.

In the F<sub>3</sub>NO plasma, NF is decomposed through the following reaction.



The species produced in the primary reactions led to secondary reactions which formed NO<sub>2</sub> ions through the following exothermic reactions:



In the case of the  $\text{NF}_3$  plasma, the above reaction is not significant because the number of O ions is remarkably small, but  $\text{F}_3\text{NO}$  causes a more significant reaction. Therefore, the number of  $\text{NF}_2$  and  $\text{NF}$  ions are fewer in the  $\text{F}_3\text{NO}$  plasma than in the  $\text{NF}_3$  plasma, whereas ions such as N,  $\text{N}_2$ , and F are present in similar amounts in the  $\text{F}_3\text{NO}$  plasma and the  $\text{NF}_3$  plasma.

In the  $\text{NF}_3$  plasma, NO ions may be generated through the bonding of O and N ions, which are etching by-products, or through a process in which N ions form Si–O–N bonding on the surface of the silicon oxide thin film [30]. In the  $\text{F}_3\text{NO}$  plasma, NO is formed by the N and O ions contained in  $\text{F}_3\text{NO}$ . In the case of  $\text{F}_3\text{NO}$ , this condition becomes the main mechanism. NO formed in this way forms  $\text{NO}_2$  through the following reaction:



In the  $\text{NF}_3$  plasma, because the number of O ions was remarkably small, this oxidation reaction occurred only to a small extent. Conversely, in the  $\text{F}_3\text{NO}$  plasma, as the number of O ions was much larger, the extent of the oxidation reaction was more significant. When the discharge power was increased, the number of NO formed was almost unchanged, but the peak of NO ions decreased due to the considerable oxidation of NO.

Figure 7 shows the  $\text{SiO}_2$  etch rate according to the discharge power and process pressure. The results imply that the lower the pressure and discharge power, the higher the etch rate of  $\text{F}_3\text{NO}$ . This is because when the pressure and discharge power is low, chemical etching occurs more easily because the number of F ions generated is greater in  $\text{F}_3\text{NO}$ . Conversely, the DC offset at a low power has a small absolute value for the  $\text{NF}_3$  and  $\text{F}_3\text{NO}$  plasmas; therefore, the ion bombardment energy does not have a significant effect on etching. When the discharge power was increased, the DC offset value of the  $\text{NF}_3$  plasma became larger than that of the  $\text{F}_3\text{NO}$  plasma, so the etch rate of  $\text{NF}_3$  also became higher. When the discharge pressure and discharge power increased, the intensity of F ions also increased as  $\text{NF}_3$  increased, so the etch rate decreased in  $\text{F}_3\text{NO}$ . Furthermore, the etch rate of silicon oxide during  $\text{F}_3\text{NO}$  plasma etching was approximately 95.0% of the rate during  $\text{NF}_3$  plasma etching.

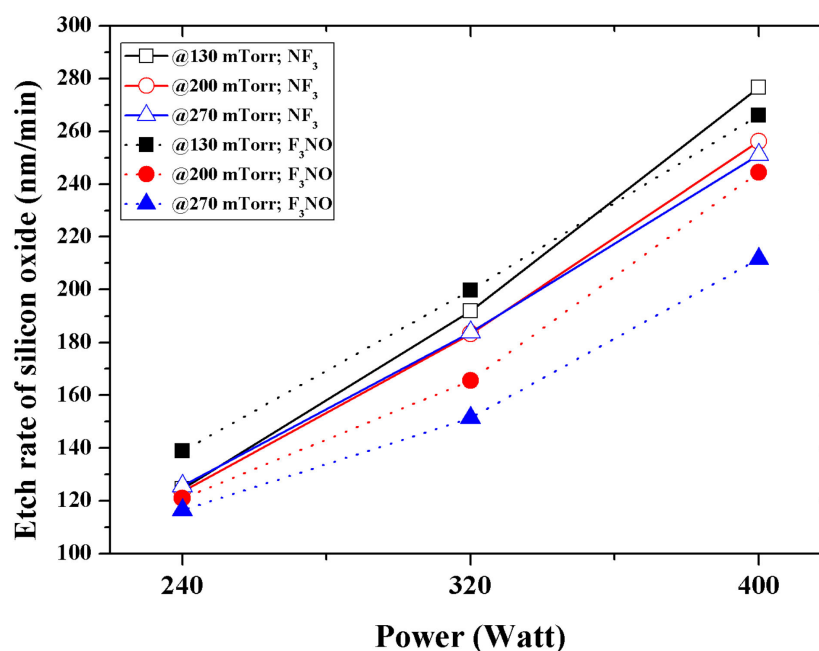
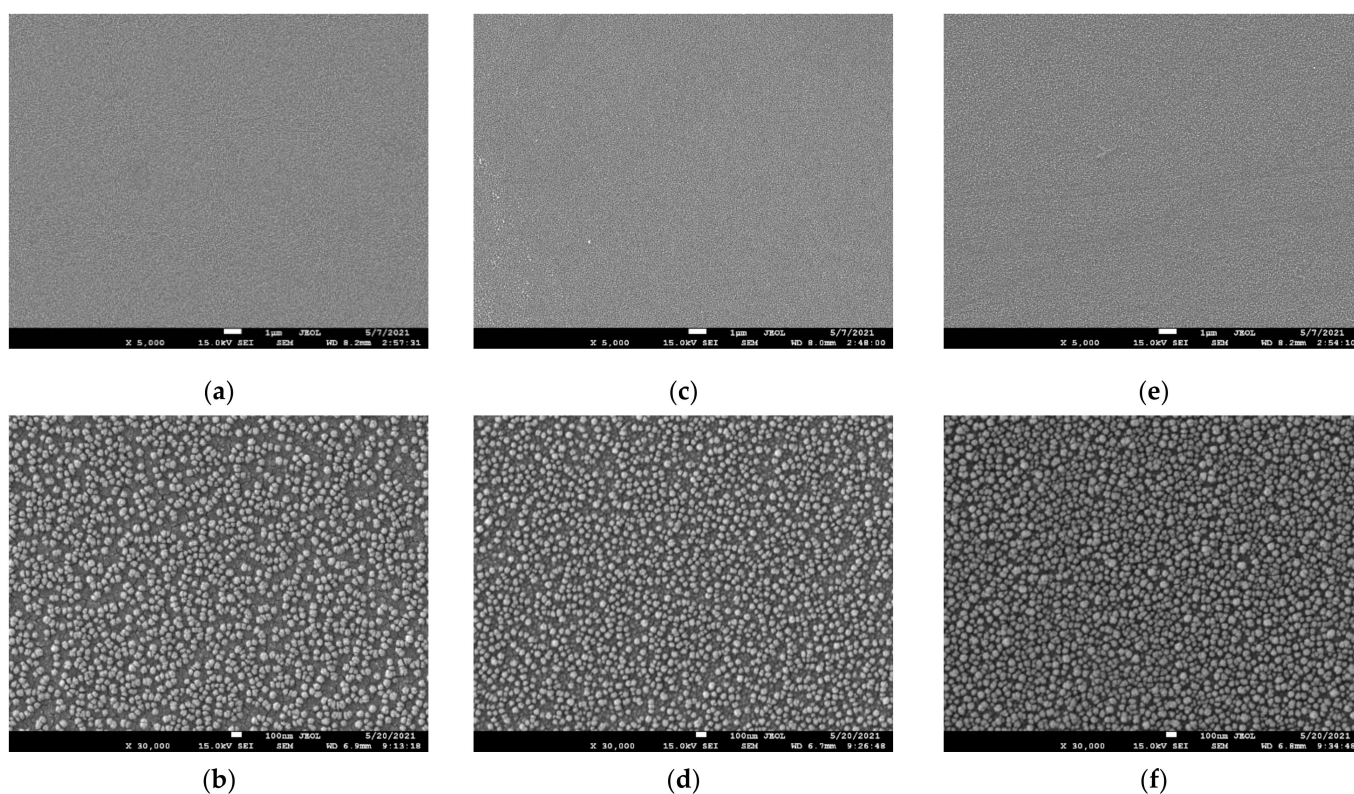


Figure 7. Etch rate as a function of input for various working pressures during plasma silicon oxide etching at a total flow rate of 120 sccm.

We performed SEM measurements to determine whether O or N ions present in the plasma had a negative effect on the etching quality. Figure 8 shows a SiO<sub>2</sub> surface of SEM images after the etching process at 400 W discharge power and 270 mTorr pressure. For accurate SEM measurements, a platinum coating was applied on the surface by sputtering. The round shape particles in the figures are platinum nanoparticles from the platinum coating. The size of these nanoparticles is in order of several nanometers. Besides platinum nanoparticles, no other structures such as cracks or holes were found on the surface. No significant difference was observed between the SEM images of the unprocessed and processed surface of SiO<sub>2</sub>. Therefore, it was confirmed that O or N ions in F<sub>3</sub>NO did not have a negative effect on the etching quality.



**Figure 8.** Surface of the SEM images of the SiO<sub>2</sub> samples: without etching of (a)  $\times 5000$ , (b)  $\times 30,000$ , at 400 W discharge power and 270 mTorr process pressure with NF<sub>3</sub> plasma of (c)  $\times 5000$ , (d)  $\times 30,000$  and F<sub>3</sub>NO plasma of (e)  $\times 5000$  and (f)  $\times 30,000$ .

Figure 9 shows EDS spectra of the SiO<sub>2</sub> surface without process and after etching at a 400 W discharge power and 270 mTorr pressure with the NF<sub>3</sub> and F<sub>3</sub>NO plasmas. The C peak in the EDS spectra was caused either by carbon contamination or by the window in the detector. Except for carbon and platinum (from the platinum coating), no peaks other than O and Si were found in the EDS spectra. This indicates that nitrogen, oxygen, or NO did not chemically contaminate the SiO<sub>2</sub> surface during the etching process.

The mass ratio of silicon and oxygen is noticeable in the EDS spectra. The mass ratio of silicon and oxygen on the SiO<sub>2</sub> surface is almost the same when the process is not performed and when the NF<sub>3</sub> etching process is performed. However, the mass ratio of O appears less on the SiO<sub>2</sub> surface after F<sub>3</sub>NO etching. This may be caused by the following reaction on the SiO<sub>2</sub> surface during F<sub>3</sub>NO etching.





As above, NO ions absorb O in the SiO<sub>2</sub> surface to decrease surface oxidation [31]. Therefore, the F<sub>3</sub>NO etched SiO<sub>2</sub> surface has a smaller oxygen mass ratio than the NF<sub>3</sub> etched SiO<sub>2</sub> surface. Moreover, this de-oxidation process increases the Si etching rate, especially during etching with F<sub>3</sub>NO at low pressure and low power with a significant quantity of NO ions.

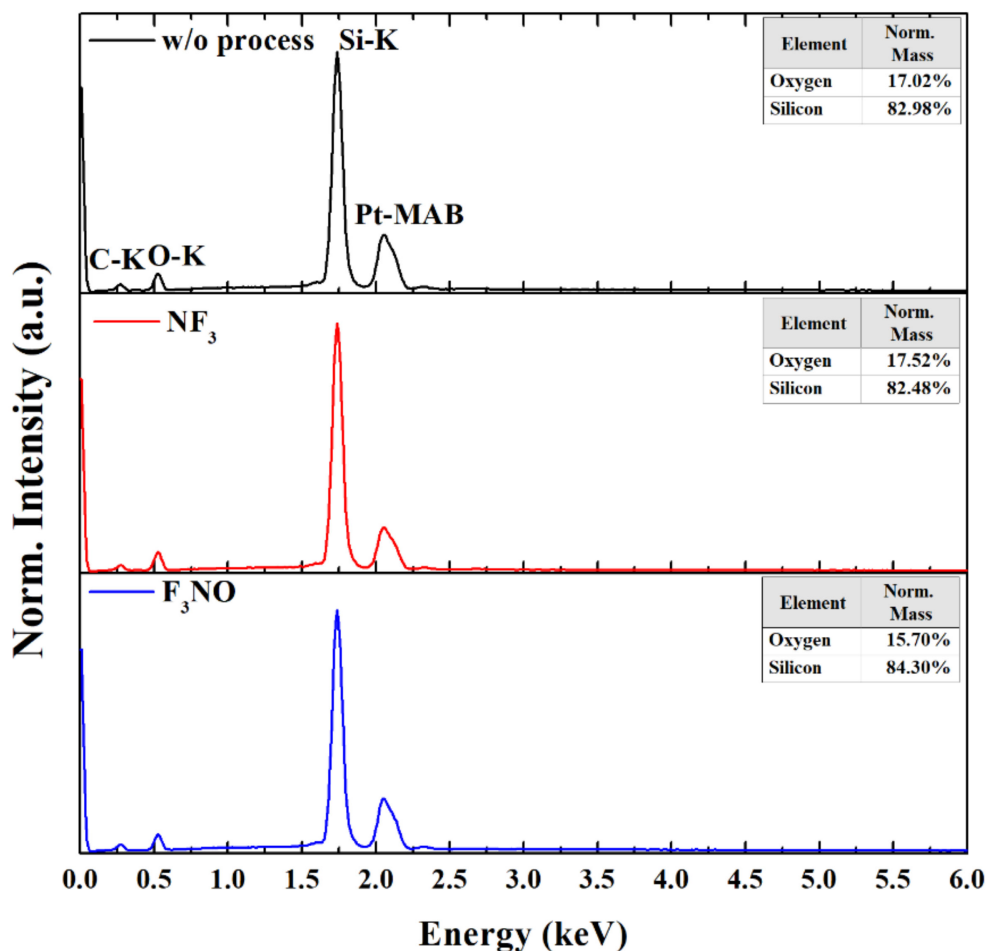


**Figure 9.** EDS spectra of the SiO<sub>2</sub> surface without etching, at 400 W discharge power and 270 mTorr process pressure with NF<sub>3</sub> plasma and F<sub>3</sub>NO plasma.

#### 4. Conclusions

The DC offset was measured during NF<sub>3</sub> and F<sub>3</sub>NO plasma discharges. Compared with the DC offset of the NF<sub>3</sub> plasma, the F<sub>3</sub>NO plasma showed an almost similar DC offset value. This finding confirms that the F<sub>3</sub>NO plasma, similar to the NF<sub>3</sub> plasma, can have a very high electronegativity. Moreover, the NF<sub>3</sub> plasma, similar to the F<sub>3</sub>NO plasma, may also exhibit unstable or non-uniform characteristics. Therefore, the diluent of an inert gas into the F<sub>3</sub>NO plasma can be effective.

The ions generated in the NF<sub>3</sub> plasma and the F<sub>3</sub>NO plasma during the etching of the SiO<sub>2</sub> thin film were measured through the RGA. In the case of F ions, when the discharge power and discharge pressure were low, more F<sub>3</sub>NO plasmas were generated than NF<sub>3</sub> plasmas. The result was the same for the etching by-products (SiF, SiF<sub>2</sub>, and SiF<sub>3</sub>). In addition, as the power increased, the intensity of F ions in NF<sub>3</sub> rapidly increased, whereas in the F<sub>3</sub>NO plasma, the ions of F gradually increased even if the discharge power of F increased. This result showed a similar trend for other ions afterward, implying that the plasma density of F<sub>3</sub>NO reacts more slowly to the change of the discharge power compared to NF<sub>3</sub>. Ions O and O<sub>2</sub> generated during the plasma discharge were much more significant in the F<sub>3</sub>NO plasma than in the NF<sub>3</sub> plasma, which is attributed to the O ions contained in

$F_3NO$ . Furthermore, the intensity of O ions can affect the etching mechanism of the  $F_3NO$  plasma.  $F_2$ , N,  $N_2$  ions occur more in  $F_3NO$  at a low discharge power and occur more in  $NF_3$  at a high discharge power. In contrast,  $NF_2$  ions are much higher in  $NF_3$  ions under all conditions. O ions in  $F_3NO$  cause a reaction to decompose  $NF_2$ . When the discharge power is low, the NO ions of  $F_3NO$  are generated in higher amounts compared to the  $NF_3$  plasma. However, as the discharge power increases, the number of NO ions in  $F_3NO$  gradually decreases, whereas the NO ions in the  $NF_3$  plasma rapidly increase, and the intensity of the peak of NO generated in  $F_3NO$  becomes almost similar. Conversely,  $NO_2$  ions occur more in the  $F_3NO$  plasma under all conditions. In the  $F_3NO$  plasma, many NO ions are generated in the process of decomposing  $NF_2$ . However, when the pressure increases, NO ions are oxidized by O ions to form  $NO_2$  ions, and thus the number of NO ions decreases. Through this oxidation reaction, many more  $NO_2$  ions are generated in the  $F_3NO$  plasma than in the  $NF_3$  plasma.

The  $SiO_2$  etch rates of the  $NF_3$  and  $F_3NO$  plasmas were compared. The results show that the lower the pressure and discharge power, the higher the etch rate of  $F_3NO$ . This is because the intensity of F ions is higher in the  $F_3NO$  plasma at low pressure. As the discharge power increases, the intensity of F ions in the  $NF_3$  plasma increases. Therefore, the etch rate of the  $NF_3$  plasma increases. The etch rate of silicon oxide during  $F_3NO$  plasma etching was approximately 95.0% of the  $NF_3$  plasma etching rate.

To compare the etch qualities, SEM measurements were performed. There was no difference between the unetched and etched  $SiO_2$  surface with the  $NF_3$  and  $F_3NO$  plasmas. Therefore, we found that N or O ions in  $F_3NO$  did not negatively affect the etch quality. The results of this study confirm the cleaning properties of  $F_3NO$ . Nonetheless, the limitation of this study is that only  $NF_3$  and  $F_3NO$  plasmas were compared. In addition, EDS measurements were performed in parallel to assess the possibility of chemical contamination of the surface by ions in  $F_3NO$  and phenomena occurring on the  $SiO_2$  surface during etching. As a result of the measurement, no chemical contamination was observed during etching with  $NF_3$  plasma or  $F_3NO$ . Unlike  $NF_3$  plasma etching, it was observed that the mass ratio of oxygen of the  $SiO_2$  surface decreased during  $F_3NO$  plasma etching. This may be attributed to the de-oxidation process of the  $SiO_2$  surface by NO ions.

The characteristics of the  $F_3NO$  plasma were identified through these results, and the potential for replacing  $F_3NO$  with  $NF_3$  was confirmed. Further studies will be needed when inert gases, such as Ar or He, are used as diluent. In addition, higher pressures need to be evaluated for the cleaning ability.

**Author Contributions:** Conceptualization, M.-H.K., J.-H.K. (Jung-Hun Kwak) and G.-C.K.; methodology, W.-J.K., H.-T.K. and G.-W.S.; validation, H.-T.K. and J.-H.K. (Ji-Hwan Kim); formal analysis, W.-J.K., I.-Y.B. and G.-W.S.; investigation, I.-Y.B., J.-H.K. (Ji-Hwan Kim), Y.-S.P. and Y.C.; resources, M.-H.K., Y.C. and B.-H.K.; data curation, I.-Y.B. and Y.-S.P.; writing—original draft preparation, W.-J.K.; writing—review and editing, W.-J.K.; supervision, G.-C.K. All authors have read and agreed to the published version of the manuscript.

**Funding:** This research was supported by the Korea Institute of Energy Technology Evaluation and Planning (KETEP) and the Ministry of Trade, Industry & Energy (MOTIE) of the Republic of Korea (No. 20172010104840). The present Research also has been conducted by the Research Grant of Kwangwoon University in 2019.

**Institutional Review Board Statement:** Not applicable.

**Informed Consent Statement:** Not applicable.

**Data Availability Statement:** Data available on reasonable request.

**Conflicts of Interest:** The authors declare no conflict of interest.

## References

1. Arnold, T.; Harth, C.M.; Mühle, J.; Manning, A.J.; Salameh, P.K.; Kim, J.; Weiss, R.F. Nitrogen trifluoride global emissions estimated from updated atmospheric measurements. *Proc. Natl. Acad. Sci. USA* **2013**, *110*, 2029–2034. [[CrossRef](#)] [[PubMed](#)]
2. Golja, B.; Barkanic, J.A.; Hoff, A. A review of nitrogen trifluoride for dry etching in microelectronics processing. *Microelectron. J.* **1985**, *16*, 5–21. [[CrossRef](#)]
3. Donnelly, V.M.; Flamm, D.L. Dautremont-Smith WC and Werder DJ. *J. Appl. Phys.* **1984**, *1984*, 55.
4. Bruno, G. Study of the NF<sub>3</sub> plasma cleaning of reactors for amorphous silicon deposition. *J. Vac. Sci. Technol. A* **1994**, *12*, 690–698. [[CrossRef](#)]
5. Langan, J.G. Electrical impedance analysis and etch rate maximization in NF<sub>3</sub>/Ar discharges. *J. Vac. Sci. Technol. A* **1998**, *16*, 2108–2114. [[CrossRef](#)]
6. Raoux, S.; Tanaka, T.; Bhan, M.; Ponnekanti, H.; Seamons, M.; Deacon, T.; Xia, L.-Q.; Pham, F.; Silveti, D.; Cheung, D.; et al. Remote microwave plasma source for cleaning chemical vapor deposition chambers: Technology for reducing global warming gas emissions. *J. Vac. Sci. Technol. B Microelectron. Nanometer Struct.* **1999**, *17*, 477. [[CrossRef](#)]
7. Ji, B.; Elder, D.L.; Yang, J.H.; Badowski, P.R.; Karwacki, E.J. Power dependence of NF<sub>3</sub> plasma stability for in situ chamber cleaning. *J. Appl. Phys.* **2004**, *95*, 4446–4451. [[CrossRef](#)]
8. Martin, A.A.; Toth, M. Cryogenic electron beam induced chemical etching. *ACS Appl. Mater. Inter.* **2014**, *6*, 18457–18460. [[CrossRef](#)] [[PubMed](#)]
9. Martin, A.A.; Aharonovich, I.; Toth, M. Gas-Mediated Electron Beam Induced Etching - From Fundamental Physics to Device Fabrication. *Microsc. Microanal.* **2014**, *20*, 364–365. [[CrossRef](#)]
10. Volynets, V.; Barsukov, Y.; Kim, G.; Jung, J.E.; Nam, S.K.; Han, K.; Kushner, M.J. Highly selective Si<sub>3</sub>N<sub>4</sub>/SiO<sub>2</sub> etching using an NF<sub>3</sub>/N<sub>2</sub>/O<sub>2</sub>/H<sub>2</sub> remote plasma. I. Plasma source and critical fluxes. *J. Appl. Phys.* **2020**, *38*, 023007. [[CrossRef](#)]
11. Woytek, A.J.; Lileck, J.T.; Barkanic, J.A. Nitrogen trifluoride—A new dry etchant gas. *Solid State Technol.* **1984**, *27*, 172–175.
12. Myhre, G.; Shindell, D.; Pongratz, J. Anthropogenic and natural radiative forcing. *Anthropog. Nat. Radiat. Clim. Chang.* **2014**, 659–740.
13. Kim, H.S.; Kim, E.Y.; Lee, P.S. Study of the enrichment of NF<sub>3</sub> waste gas using zeolite and polymeric membranes. *Sep. Purif. Technol.* **2019**, *220*, 1–7. [[CrossRef](#)]
14. Tasaka, A. Electrochemical synthesis and application of NF<sub>3</sub>. *J. Fluor. Chem.* **2007**, *128*, 296–310. [[CrossRef](#)]
15. Weiss, R.F.; Mühle, J.; Salameh, P.K.; Harth, C.M. Nitrogen trifluoride in the global atmosphere. *Geophys. Res. Lett.* **2008**, *35*. [[CrossRef](#)]
16. Wieland, R.; Pittroff, M.; Boudaden, J.; Altmannshofer, S.; Kutter, C. Environmental-friendly fluorine mixture for CVD cleaning processes to replace C<sub>2</sub>F<sub>6</sub>, CF<sub>4</sub> and NF<sub>3</sub>. *ECS Trans.* **2016**, *72*, 23. [[CrossRef](#)]
17. Hellriegel, R.; Hintze, B.; Winzig, H.; Albert, M.; Bartha, J.W.; Schwarze, T.; Pittroff, M. Feasibility study for usage of diluted fluorine for chamber clean etch applications as an environmental friendly replacement of NF<sub>3</sub>. *MRS Online Proc. Libr.* **2006**, 914. [[CrossRef](#)]
18. Yonemura, T.; Fukae, K.; Ohira, Y.; Mitsui, Y.; Takaichi, T.; Sekiya, A.; Beppu, T. Evaluation of FNO and F<sub>3</sub>NO as Substitute Gases for Semiconductor CVD Chamber Cleaning. *J. Electrochem. Soc.* **2003**, *150*, G707–G710. [[CrossRef](#)]
19. Kwon, H.-T.; Kim, W.-J.; Shin, G.-W.; Lee, H.-H.; Lee, T.-H.; Kang, M.-H.; Kwon, G.-C. Plasma Etching of Silicon at a High Flow and a High Pressure of NF<sub>3</sub> in Reactive Ion Etching. *J. Korean Phys. Soc.* **2019**, *74*, 1135–1139. [[CrossRef](#)]
20. Kihara, T.; Yokomori, K. Simultaneous measurement of refractive index and thickness of thin film by polarized reflectances. *Appl. Opt.* **1990**, *29*, 5069–5073. [[CrossRef](#)]
21. Sobolewski, M.A.; Langan, J.G.; Felker, B.S. Electrical optimization of plasma-enhanced chemical vapor deposition chamber cleaning plasmas. *J. Vac. Sci. Technol. B* **1998**, *16*, 173–182. [[CrossRef](#)]
22. Pruette, L. Evaluation of a Dilute Nitrogen Trifluoride Plasma Clean in a Dielectric PECVD Reactor. *Electrochem. Solid-State Lett.* **1999**, *2*, 592. [[CrossRef](#)]
23. Entley, W.R.; Langan, J.G.; Felker, B.S.; Sobolewski, M.A. Optimizing utilization efficiencies in electronegative discharges: The importance of the impedance phase angle. *J. Appl. Phys.* **1999**, *86*, 4825–4835. [[CrossRef](#)]
24. Steinfeld, J.I. Reactions of photogenerated free radicals at surfaces of electronic materials. *Chem. Rev.* **1989**, *89*, 1291–1301. [[CrossRef](#)]
25. Donnelly, V.M.; Flamm, D.L.; Dautremont-Smith, W.C.; Werder, D.J. Anisotropic etching of SiO<sub>2</sub> in low-frequency CF<sub>4</sub>/O<sub>2</sub> and NF<sub>3</sub>/Ar plasmas. *J. Appl. Phys.* **1984**, *55*, 242–252. [[CrossRef](#)]
26. Langan, J.G.; Rynders, S.W.; Beck, S.E.; Felker, B.S. The role of diluents in electronegative fluorinated gas discharges. *J. Appl. Phys.* **1996**, *79*, 3886. [[CrossRef](#)]
27. Reyes-Betanzo, C.; Moshkalyov, S.A.; Ramos, A.C.S.; Swart, J.W. Mechanisms of silicon nitride etching by electron cyclotron resonance plasmas using SF<sub>6</sub>-and NF<sub>3</sub>-based gas mixtures. *J. Vac. Sci. Technol. A* **2004**, *22*, 1513. [[CrossRef](#)]
28. Nahomy, J.; Ferreira, C.M.; Gordiets, B.; Pagnon, D.; Touzeau, M.; Vialle, M. Experimental and theoretical investigation of a N<sub>2</sub>-O<sub>2</sub>DC flowing glow discharge. *J. Phys. D Appl. Phys.* **1995**, *28*, 738–747. [[CrossRef](#)]
29. Guerra, V.; Loureiro, J. Non-equilibrium coupled kinetics in stationary N<sub>2</sub>-O<sub>2</sub> discharges. *J. Phys. D Appl. Phys.* **1995**, *28*, 1903–1918. [[CrossRef](#)]

- 
30. Kim, D.J.; Yun, Y.B.; Hwang, J.Y.; Lee, N.E.; Kim, K.S.; Bae, G.H. Role of N<sub>2</sub> during chemical dry etching of silicon oxide layers using NF<sub>3</sub>/N<sub>2</sub>/Ar remote plasmas. *Microelectron. Eng.* **2007**, *84*, 560–566. [[CrossRef](#)]
  31. Barsukov, Y.; Volynets, V.; Lee, S.; Kim, G.; Lee, B.; Nam, S.K.; Han, K. Role of NO in highly selective SiN/SiO<sub>2</sub> and SiN/Si etching with NF<sub>3</sub>/O<sub>2</sub> remote plasma: Experiment and simulation. *J. Vac. Sci. Technol. A* **2017**, *35*, 61310. [[CrossRef](#)]